N0850002

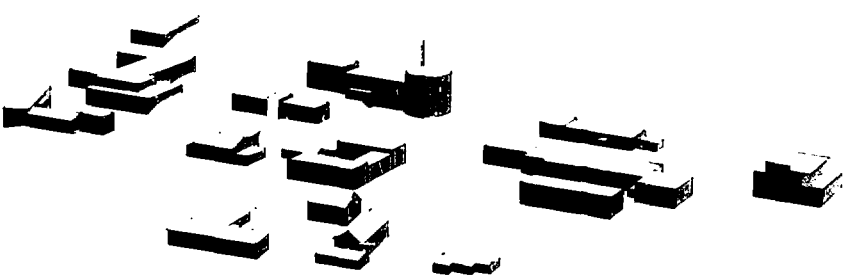

Institute for
energy technology

IFE/KR/E-84/008

VACUUM SPARK BREAKDOWN MODEL BASED ON EXPLODING METAL WIRE PHENOMENA

by

John Haaland

ISSN-0333-2039
ISBN-82-7017-060-7

June, 1984
Institute for Energy Technology, Kjeller, Norway

TABLE OF CONTENTS

Section	Page
1. Introduction	1
2. Pre breakdown processes related to interactions at the electrodes	3
3. Pre-breakdown model for the vacuum spark	6
4. Comparisons with experimental findings reported in litterature	7
5. Discussion	11
6. Conclusion	13
7. References	14
8. comments to the figures	16

SUMMARY

Spark source mass spectra (SSMS), indicates that ions are extracted from an expanding and decaying plasma. The intensity distribution shows no dependance on vaporization properties of individual elements which indicates explosive vapour formation. This seems further to be a requirement for bridging a vacuum gap. A model including plasma ejection from a superheated anode spot by a process similar to that of an exploding metal wire is proposed. The appearance of hot plasma points in low inductance vacuum sparks can then be explained as exploding micro particles ejected from a final central anode spot.

The phenomenological model is compared with available experimental results from litterature, but no extensive quantification is attempted.

1. Introduction

In Spark Source Mass Spectrography (SSMS), remarkably simple spectra are obtained from a radio frequency vacuum spark source on a photoplate detector. The intensity distribution is dominated by single charged elemental ions, and with a weakening factor of 5-10 to successive higher ionization stages. Molecular ions from monoxides and low molecular aliphates are never multicharged, and this is also the case with the long cluster series sometimes formed by the lighter group four elements. See figure 1 with text.

This apparent spectral simplicity led one at first to assume that mass line intensities varied proportional to corresponding elements concentrations within a factor of two. Much larger deviations were found in many cases which further led to experimental determination of individual relative sensitivity factors (RSF's) based on standardized materials. Suitable standards are not always obtainable, and several formulas have been proposed which relates measured line intensities to corresponding elemental concentrations /1/. The formulas depends on various combinations of heats of sublimation, melting and boiling points, first ionization potentials, ionic ratios and total ionization cross sections. These formulas seem not related to any specific model describing the processes taking place in the ion source.

Although vacuum spark discharges have been investigated for a very long time, the transient processes leading to breakdown of the gap is still not fully understood. Vacuum means in this connection an ambient pressure where the free length of path of individual particles by far exceeds gap dimensions. This means no particle collissions and that the plasma producing processes initially are confined to the electrode surfaces. Breakdown means a plasma production sufficient to make an initially dielectrically resistive gap conducting to such an extent that the current is limited by the external circuit only.

W. Lochte-Holtgreven investigated radiation from plasmas produced by exploding wires some thirty years ago. He found similarities to the

emission from vacuum and sliding sparks and proposed that studies of exploding wires could give the key to the vacuum spark processes as well. At a first look one difference is striking : The vacuum gap has to be filled with plasma to a certain density to make it conducting, whereas the metal wire of solids density must first be vaporized and the plasma density reduced further to a point where excitation and ionization grows.

A wire explosion is a transient process where a large amount of electron energy is forced through a metal wire of small cross section in the shortest possible span of time. According to conditions, the explosion may be termed slow, fast or ablative. In any case, the current rise initially to a maximum and then falls rapidly to near zero and remains there for a short period (dwell) until it again raises abruptly in the explosive phase. There are several hypotheses on what goes on within the wire during the fast current rise /2/. One hypothesis suppose normal heating up to the melting point. From then on inertial forces and selfmagnetic compression hinder the further expansion to an extent where the relationship between resistance and energy uptake become anomaleous and no longer obey Ohms law. The liquid become superheated to temperatures far beyond the vaporization point. This unstable liquid undergoes a sudden phase change to a more stable two-phase system where metal droplets are immersed in a dense gaseous phase. The current drops abruptly due to particle separations in the gas phase, but increase again upon further expansion and formation of a conducting plasma. The ionization is negligible in the highly compressed gas phase which emits practically no radiation, and the dwell is a dark period as well. This simple hypothesis explain the observed drop in corrent rise (dI/dt), and the formation of spherical metal droplets a few microns in diameter which can be collected from a screen placed in the neighbourhood of the wire during explosion.

In vacuum sparks, normally two or three drops in the current rise - analogues to the one observed during a wire explosion - are found at regular intervals during the prebreakdown phase. Each individual drop is linked to a plasmaproducing energy dump process located to one or

more random spots in the anode tip. Anode spots are formed as a result of focused field emitted electron bursts from cathode.

These processes will be further outlined in the next chapter. Then follows a chapter where the filling of the vacuum gap with plasma is modelled as a cooperative action of specific cathode and anode processes, and finally a chapter where the proposed model is compared with experimental results collected from litterature.

Since the amount of energy dissipated per unit area and time (watt/cm^2) is a deciding quantity, fast circuits are required to reach high plasma temperatures and ionization stages. Low inductance (10-100 nH) vacuum sparks gives surprisingly high ionization stages requiring energies corresponding to voltages orders of magnitude higher than the gap voltage. B. Edlén investigated isoelectronic spectra from highly stripped heavy atoms up to molybdenum in similar vacuum sparks forty years ago. Similar plasmas from exploding wires have only been produced in recent years due to action of very short (10-30 ns) bursts of relativistic electrons /3/.

The high ion production from a low induction vacuum spark would destroy focus in a mass spectrograph. A.J. Depster /4/ connected the electrodes to the secondary of a Tesla coil and obtained a high frequency (0.5 MHz) low energy spark source suitable for SSMS work. The general characteristic of an expanding plasma wave is retained despite the high frequency, and the first ionization stage dominates as shown on figure 1. The consequences for the SSMS method will be further outlined in a following report based on earlier work /5/.

2. Pre breakdown processes related to interactions at the electrodes

The initial flow of current is due to field emission of electrons from the cold cathode surface. Field enhancements, probably by a factor of 100 near the tips of microprotrusions or whiskers are generally agreed upon to bring the observed electron emission in accordance with the

Fowler-Nordheim eqation. This current may heat the whiskers and produce thermionic emitted electrons in addition. Both heating and cooling effects may coexist depending on individual work functions, but the general trend is a heating that ends in destruction of the whisker and explosive emission of a microplasma jet.

The field emitted electrons are accellerated as they fall through the gap voltage, but with individual components of transverse movements from the initial short range accellerations through respective whisker fileds. The resulting trajectories are thus parabolic.

Secondary electrons are emitted form the cathode when positive ions approach whisker tips. Multiple charged ions may be very effective in this respect. Photoemission become important in later prebreakdown stages due to intense uv- and x-radiation. Ions and neutrals evaporated from cathode whiskers, along with the electron emission, create a stationary sheath at the surface. As the whiskers heats up and resistance increases, it is reasonable to assume that the emission is averaged over the individual whiskers and that the activities become correlated in time. A resulting collective explosion of several cathode whiskers could produce the fast anode directed plasma jet of the type actually observed /6/. This high current dense plasma jet is z-pinched in direction to anode. The slower electrons are trapped by ions, and the plasma undergo oscillations which grow in the pinch direction. The faster run away electrons are accellerated and hit a central spot on anode as a pencil like beam.

Whiskers, similar to those at the cathode, but positively charged are simultaneously formed at anode surface. Cathode emitted electrons are focused onto the individual tips and cause a filamentation in the electron beam. Field evaporated ions and clusters from the heated whiskers support this filamentation. Together with the release of absorbed surface layers, they form a slow moving cathode directed plasma wave. The evaporated ions and ionized neutrals cause a sharp reduction in the anode fall of potential at the locations of emitting whiskers due to space charge neutralization. These reductions in vol-

tage drop causes more current to flow into this local anode areas to heat the whiskers further up. This lead to further evaporation and ionization, and again an increase in electron corrent by a runaway process leading to pinching and anode spot formation /21/. The anode spot formation is analogous to the exploding wire process described earlier in that an energetic electron burst heats a piece of anode material with a very small cross section to become a superheated liquid. Simultaneously with a collective explosion of anode spots a drop in the current increase waveform can be registered. This feature shows some complexity, but consits essentially of a dip and a peak from an associated current burst. A second feature is detected on the dI/dt curve approximately 0.5 microsec later in the case of a low inductance vacuum spark, when the above mentioned fast cathode plasma jet hits a central spot on anode. A fast and dense plasma jet expands in direction of cathode and bridge the gap when it merges with the cathode plasma.

The main part of the electron beam energy is used for vapor production, whereas negligible amounts are radiated or conducted away /8/.

The radiation from spark plasmas and particularly from anode, shows a complex picture involving the whole spectrum from microwaves to hard x-rays. Micro waves are due to plasma oscillations primarily in the fast anode directed strimer (K-band), and in the dense cathode directed jet from the central anode spot (X-band). Soft x-ray scontinuum and characteric Kα,β from the entire anode surface are due to electron bursts from cathod accellerated through the gap. Characteristic x-radiation from multiply changed ions are due to induced voltage peaks which far exceeds gap voltag and probably can be associated wsith the dI/dt dips. Hard x-rays from highly stripped ions are located to the explosion of charged particles emitted from the central anode crater.

3. Pre-breakdown model for the vacuum spark

In this chapter is proposed a phenomenological model based on experimental evidences to explain the necessary filling of the insulating vacuum gap with a conducting plasma during the pre-breakdown period. The plasma production cannot be the result of a steady evaporation from electrode surface as this material would expand away into ambient vacuum with no possibility to bridge the gap. The processes must be very fast and able to produce dense plasmas as is the case for exploding metal wires. The collective cathode whisker explosions at t_2 (Figure 2) may probably be considered as slow, whereas the explosions on anode at t_1 and t_3 may be fast and ablative respectively. The pre-breakdown process as a whole can be considered as a chain of concecutive cathode and anode processes which cooperate in filling the vacuum gap with plasma. Further, it is the fields (F) at the emission centers on cathode surface that is of importance rather than gap voltages (V).

$$F = \beta(V/d)$$

where d is electrode distance and β the field magnification factor ($\approx 10^2$).

Figure 2 illustrates the filling up with plasma where the consecutive processes are resolved in time and position. Starting at t_0, field emitted electrons release a slow moving plasma (A_0) from absorbed layers on anode surface along with field evaporated ions and clusters from whiskers heated by focused electrons. A stationary double layer (K_0) cover the cathode surface. At t_1 the anode whiskers melts and become superheated. A dip in the dI/dt curve can be noticed, and a fast (10^6 cm/sec) plasmawave A_1 expands toward cathode. As it approaches and hits the cathode at t_2, a very fast (10^7 cm/sec) streamer is formed by collective explosions of cathode whiskers. The current densitty is high, and no longer carried by electrons alone. The streamer become z-pinched toward anode, and undergo stable plasma oscillations. When the pencil of energetic electrons penetrates anode

at t_3, a second dip can be noticed and a very dence plasma wave (10^6 cm/sec) expands toward cathod and fill the gap as it meets the cathode plasma at t_4. The cathode plasma production may be intensified by photoemission and -ionization.

Along with, and in front of the dens plasma (A_2), charged particles which form hot plasma points on explosion are somet mes observed.

4. Comparisons with experimental findings reported in litterature

D.J. DeGeeter /7/ investigated the formation of anode spots microscopically. The anode and cathode were 1 1/2 in. diam molybdenum and stainless steel spheres respectively, and with a gap spacing of 0.42 mm. On increasing the voltage to approximately 60-70 kV, several areas on the anode started glowing. At a further slow increase in voltage, an increasing number of up to thirty individual spots with typical diameters of 0.05 mm were observed. This spot formation was reversible, but occasionally and suddenly one or more of these bluish spots developed into larger and very luminous spots. These last events were irreversible and led to breakdown directly. The onset was very sharp, indicating that the cathode emitted electron current was very sensitive to changes in voltage and field according to the Fowler-Nordheim equation. The reversible bluish spots were not real in that they most often become cleaned up. This is evident from experiments were lateral movements of cathode with respect to anode at a constant gap spacing cause the entire pattern of anode spots to move across the anode /18/. This indicates again that anode whiskers initiates the necessary electron focusing and bundeling, but do not themselves represent real anode spots.

The irreversible (explosive) formation of the larger luminous spots corresponds to the process at t_1 on Figure 2. Not all sparks could be traced to a specific luminous spot, and the actual break down could as well be described to formation of a central spot at t_3. These events cannot be distinguished in the experiments due to the short cross over times for A_1 and K_1 (Figure 2).

The electron energy dumped in anode spots at t_1 (and t_3) devides between the time dependent explosive formation of a plasma wave, the crater formation by Joule heating and the radiation. At the fast current rises during spot formation, the explosive ejection of plasma is the prime loss mechanism of anode power. The temperature in the central spot just after the explosion at t_3 is found to be closely related to the boiling point of anode material /8/. The crater dimension increases considerably for low melting and easily destructable materials. The spots formed at t_1 were most often cleaned up as explained above.

Lee et al. /6/ found the time interval between three dips on the dI/dt curve to be approximately 0.5 microsec. (figure 7). Negus et al. /16/ using a slightly different apparaturs found always two x-ray bursts with simultaneous dI/dt dips corresponding to t_1 and t_3 and with constant interval of 0.4 microsec. (Figure 13). This constancy indicates a close connection with cross over times for specific particle beams (A_1 and K_1) and that the process leading to a dI/dt dip is confined to an electrode (anode) surface. At very short electrode distances ($\approx 10^3$ Å) and 10-40 V, a cathode field emission in excess of 10^7 A/cm^2 forms a pit on anode within 0.1 microsec. /19/. The high pressure vapor ejected during the pure electron heating emits continuous radiation similar to an exploding wire confined in a narrow tube. A single drop in the current rise was observed.

The triggered low inductance vacuum spark has been studied extensively in recent years, particularly due to the discovery of hot plasma points above the anode tip. They are detected toward end of the pre-breakdown period as they emits hard x-rays from inner shell transitions in highly stripped atoms. The electrical parameters and electrode gap spacings for the experiments cited below are summarized in the following table.

Table II. Electrical parameters and gap spacings in low inductance vacuum spark experiments.

kV	F	nH	Gap mm	Reference
19	13	160	3	Cohen (1968) /11/
14	15	80	5	Lee (1971) /6/
16	15	80	6	Fraekel (1972) /12/
10	30	23.6	8	Cilliers (1975) /9/
18-14	19	40	5	Negus (1979) /16/
15	10	60	4-7	Veretennikov (1981) /10/

Chen et al /11/, Figure 3, and Fraenkel et al /12/, Figure 5, obtained pin hole x-ray photographs and estimated the diameters to be at most a few microns. These hot spots were later located also to other positions in the gap, as well in the neighbourhood of cathode as offaxis by Negus et al. /16/, Figure 14. They estimated the particle density in the hot plasma points to be 10^{21}-10^{22} cm^{-3}. Welch et al. /20/ found the plasma point images to be elongated with a penumbra surrounding a more dence central region. Comparing the elongation with an estimated lifetime of 10^{-8} sec., they found the plasma point to be moving at 10^{6} cm/sec.

Lee /6/ and /15/, Figure 9, observed the hot plasma points in front of a fast moving plasma layer released from the anode tip at a velosity of 10^{6} cm/sec. This is in agreement with Welch et al. /20/, and compares well with the model on Figure 2 where the combined emission is denoted by A_2 and the broken arrow.

Veretennikov et al. /10/ and Figure 17, found that the minimum pinch radius (r) in the plasma constriction occurred 25 nanosec before the dI/dt dip and the x-ray bursts. The emission of characteristic Kα from Fe II-XV coincides with the beginning of the hard x-ray emission at hν > 100 keV due to the induced high voltage peak. After still 5 nanosec follows the emission of the helium-like Fe XXV resonnant lines and the emission of x-rays at 25-100 keV. This result is in fair agreement with the measurements of Cilliers et al. /9/ and Figure 10, where the hard x-ray component appeared approximately 3-5 nanosec

before the He-like lines, but do not confirm the results of Lee et al. /14/ and Figure 8, where these emission peaks coincide. The results of Veretennikov et al. compares well with the model on Figure 2 where the final pinching of K_1 might occur approximately 25 nanosec before the suprathermal electrons hits the anode and produce the dI/dt dip in current rise (dwell period). The characteristic Kα and particularly the hard x-rays at hν > 100 keV are produced toward the end of the dwell period, hard x-rays at 25-100 keV are produced in the ionizing shock wave A_2 5 nanosec later along with Fe XXV emission from positively charged microparticles that explode due to interaction with the electron emission.

It is evident from experiments (Klapisch et al. /13/, Figure 6 and Negus et al. /16/, Figure 15) that the emission from highly stripped atoms (Fe XXIV-XXV) is confined to the hot point plasmas. This radiation and the hot spots are detected only in one out of approximately three discharges, whereas the dI/dt dips appears regularly /16/. This regularity of appearance links the dI/dt dip to a primary process on the anode surface. This must be the spontaneous production of the dens plasma wave due to the stopping of a focused electron beam. The exploding microparticles may be associated with local micropinches and appears irregularly as seen on Figure 14. They may cause minor features on the dI/dt curve like those sometimes observed (Figure 17) and emit complex x-ray bursts (Figure 9).

The production of hot plasma points are quite irregular, and the responsible processes therefore secondary to the main plasma producing processes at the electrode surfaces during the per breakdown phase.

Poshekonov et al. /17/, Figure 18, has demonstrated how vacuum breakdown can be initiated by interaction of an electron beam with the anode surface. The critical dependence of intensity around 10^6 w/cm^2 indicates that specific structural changes takes place in target. The same is evident from Figure 18 where the distribution of microparticles from anode material closely resembles those collected after explosion of an electric wire.

Burkhalter et al. /3/ has demonstrated that it is possible to produce spectra quite similar to those from low inductance vacuum sparks by passing a 80 nanosec, 10^{12}w relativistic electron beam through a 50 micron Fe wire (Figure 11 and 12). The high energy disippated into the wire (50 kJ) compensate for the larger mass and longer puls compared with the spark. It is noteworthy that the x-ray emission, particularly from highly stripped atoms, are far more reproducible compared with the low inductance vacuum spark. This may be due to a closer control of conditions where the x-ray emission sites or micropinches are adhered to fixed sites along the position of the original wire. Hot plasma points (micropinches) may or may not be traced not only close to the anode, but anywhere in the gap of a low inductance vacuum spark.

5. *Discussion*

To bridge a vacuum gap and pass a high current spark, the primary process is the production of a very dense plasma jet within a very short time. By ordinary evaporation from heated electrodes, the vapours would expand away into vacuum ambient before the gap become conducting.

The plasma producing process proposed by the phenomenological model described in this report is analoguous to that of an exploding metal wire. A superheated liquid expands and become resistive upon a phase change to a more stable twophase system consisting of metal droplets immersed in a dense gas phase. The observed main dips in the dI/dt waveform is thus related to expansion of a superheated anode spot liquid caused by a pinched electron beam bombardment.

The experiments cited in the preciding chapter indicates that two or even three such process cycles are necessary to bridge the gap and make it conducting. Each cycle is assisted in plasma production by the preceding one until breakdown is completed. This explains the successive increase in energy and intesity of x-ray emission and in the amount of dense plasma produced. The observed constant delay between two dI/dt dips is related to cross over times for particle beams.

The hot plasma points which are sometimes observed, and then always at the end of the prebreakdown period, might well be exploding solid droplets ejected form a central anode spot.

Lee /15/ and Cilliers et al. /9/ ascribed the formation of hot plasma points to micropinches from electron beam heating at constrictions in emitted anode shaped plasmas, and they related the dI/dt dips to this pinch formation. Negus et al. /16/ pointed out the required unique character of such pinches to explain the explosive deposition of beam energy within the hot spot, and they did not rule out the possibility of explosion of a microparticle of solid material detached from an electrode and bombarded by ions or electrons as the formation process for hot spots. Furthermore, they collected spherical microparticles of anode material from the spark chamber walls. These particles must have been generated in a process rather than detached as random dust particles from an electrode surface.

The particle densities in the hot plasma points have been estimated to be 10^{19}-10^{22} cm^{-3}. Welch et al. /20/ found structured point plasmas with an elongated penumbra and a dense kernel which might well be of solids density.

Hot spots due to plasma instabilities and micropinches should be found at specific localizations within the gap, i.e. in the anode region where they were detected in the early experiments. Negus et al. /16/ later photographed hot spots in all parts of the gap, and even those of highest quality could be found in the cathode region. It seems therefore more probable that the observed point plasmas or hot spots are positively charged microparticles which are ejected from the central anode spot and explodes due to electron beam interaction.

Time correlations as measured between the different bursts of x-rays, microwaves and the dI/dt dips are still not conclusive. Apart from weak continuous and normal characteristic x-radiation during the whole period due to the gap voltage, the main intensity is emitted at the time of the last dI/dt dip and the central anode spot formation. Microwaves are registrated in two separate bands K (25gHz) and X

(10GHz). The K-band should probably be associated with the growing oscillations in the anode directed jet (K_1) just prior to anode spot formation. The X-band could be associated with the expanding plasma (A_2)

It seems proved that the hard x-rays (> 100 keV) from non-thermal electrons hitting the anode and forming the central spot comes a few nanosec before the resonnance radiation due to highly stripped atoms from the hot plasma points. It is also noticeable that Veretennikov et al. /10/ have registrated a pinching (of K_1) about 25 nanosec before the dI/dt dip and anode spot formation.

6. Conclusion

1. Electrical breakdown of a dielectrically resistive vacuum gap requires the formation of a sufficient amount of a plasma at a very high density and within a very short time.

2. This plasma production is similar to plasma production from explosion of thin metallic wires when short bursts of energetic electrons are forced through them.

3. The formation of an expanding superheated liquid and the simultaneous dI/dt dip in current rise prior to wire explosion is analoguous to an anode spot formation due to a pinched electron beam bombardment and a dI/dt dip in the pre breakdown period of a spark discharge.

4. If the amount of plasma produced is insufficient, it will initiate a second more efficient cycle which eventually lead to breakdown.

5. The hot spots often observed in low inductance vacuum sparks are responsible for the very high ionization stages obtained, but are of secondary importance for the breakdown to occur.

7. References

/1/ van HOYE, E., ADAMS, F. AND GIJBELS, R., Talanta, 26, 285 (1979)

/2/ CHACE, W.G. et al. eds., Exploding Wires I & II, Plenum Press, N.Y., 1959/62

/3/ BURKHALTER, P.G., DOZIER, C.M., STALLINGS, C. AND COWAN, R.D., J. Appl- Phys., 49(3), 1092 (1978)

/4/ DEMPSTER, A.J., Rev. Sci. Instr., 7, 46 (1936)

/5/ HAALAND, J., Poster pres. at XXIII CSI, Amsterdam (1983), and Int. Rep. No. IFE/I-83/013+KIK, Institute for energy technology, (1983)

/6/ LEE, T.N. AND ELTON, R.C., Phys. Rev., 3(3), 865 (1971)

/7/ DE GEETER, D.J., J. Appl- Phys., 34, 919, (1963)

/8/ COBINE, J.D. AND BURGER, E.E., J. Appl. Phys., 26, 895 (1955)

/9/ CILLIERS, W.A., DATLA, R.U. AND GRIEM, H.R., Phys. Rev. A, 12, 1408 (1975).

/10/ VERETENNIKOV, V.A., POLUKHIN, S.N., SEMENOV, O.G. AND SIDEL'NIKOV, YU.V., Sovj. J. Plasma Phys. 7, 656 (1981)

/11/ COHEN, L., FELDMAN, U., SWARTZ, M. AND UNDERWOOD, J.H., J. Opt. Soc. Am., 58, 843 (1968)

/12/ FRAENKEL, B.S. AND SCHWOB, J.L., Phys. Lett., 40A, 81, 83 (1972).

/13/ KLAPISCH, M., SCHWOB, J.L., FRAENKEL, B.S. AND OREG, J., J.

Opt. Soc. Am., 67, 148 (1977)

/14/ LEE, T.N., PROC. 2nd Top. Conf. on Puls. High-Beta Plasmas. IPP 1/127 (1972). Max Planck Inst. f. Plasma Phys. Garching bei München.

/15/ LEE, T.N., Ann. N.Y. Acad. Sci., 251, 112 (1975)

/16/ NEGUS, C.R. AND PEACOCK, N.J., CLM-P541, UKAEA (1979) Culham laboratory, Abingdon Oxfordshire, UK.

/17/ POSHEKHONOV, P.V., RYZHKOV, A.M. AND SOLOV'EV, V.I., Sov. Phys. Techn. Phys., 22, 333 (1977).

/18/ ALPERT, D., LEE, D.A., LYMAN, E.M. AND TOMASCHKE, H.E., J. Vacuum Sci. Techn., 1, 35, (1964)

/19/ BOYLE, W.S. AND GERMER, L.H., J. Appl. Phys., 26, 571 (1954)

/20/ WELCH, T.J. AND CLOTHIAUX, E.J., J. Appl. Phys., 45, 3825 (1971)

/21/ LAFFERTY, J.M., Proc. IEEE, 54, 23 (1966

8. Comments to the figures

Figure 1

SSMS mass spectra from the AEI MS 702 double focusing spectrograph with Ilford Q_2 photoplate detection of a Dempster r.f. vacuum spark ion source. In each case- a series of single spectra with graded exposures are obtained.

Figure 1 a. The sample is a metallurgical grade silicon powder with 0.6 per cent aluminium and mixed 1:1 with pure graphite powder to make the pressed electrode pins electrically conductive. Single charged ion line intensitites dominates, and the presence of much less intense multicharged ion lines are in first hand limited to the removal of the valence electrons. Al^{4+} is thus not present in the spectrum. The species present are limited to those with ionization potentials below 100 eV, and the spectral intensity distribution is closely related to the ionization potentials, This is evident from the following table giving the ionization potentials in eV for some common elements.

Table 1. Ionization potentials for some common elements in eV

	+	2+	3+	4+	5+
Al	5.97	18.8	28.5	120.0	153.6
Si	8.15	16.4	33.5	45.2	165.9
Ag	7.58	21.4	35.9	(52)	(70)
Na	5.14	47.3	71.7	98,9	138.6

Silver lines from species ionized up to five or six times can easily be traced when present as major component. The intensity ratio between single and double ionized is 5-10 for most elements, but 10^4 for sodium illustrating the exponential dependence of intensity on ionization potential.

Figure 1 b. The sample is pure Gd_2O_3 mixed 1:1 with super pure (N5) silver powder. GdO^+ is present but not GdO^{2+}. If the gadolinium oxide

had been mixed with graphite, the GdO^+ would not have been present either.

Figure 1 c. Part of a series of single charged carbon clusters with up to 21 atoms (252 mu). Such clusters are sometimes formed by the lighter group IV elements.

Figure 1 d. Normal spectrum from a plagioclas mixed with graphite 1:1.

Figure 2

A sketch indicating the time resolved axial motion of plasma waves or streamers between electrodes during the perbreakdown period. Field emitted electrons from cathode whiskers create a stationary sheath (K_0) at cathode and a slow moving streamer of adsorbed gases and evaporates from anode whiskers (A_0). Field ion evaporation from the positively charged anode whiskers initiates bundelig of the electron emission and cause a steep current increase due to space charge neutralization. The current is almost totally carried by the electrons, and the large difference in mobility between electrons and ions play an important role. At a certain time t_1 the anode whiskers melts and form a superheated liquid or dense gas phase. The arrow on top indicates an experienced dip in the current increase followed by a fast expanding plasma wave (A_1). When this wave approaches the cathode at time t_2, the field emitting cathode whiskers heats up. A combined field and thermal emission leads eventually to an explosion at t_3. A very fast, photographically detectable streamer K_1 becomes z-pinched as it approach a central spot on anode at t_3. Oscillations which grows in the pinch direction are set up in the plasma, and a pencil shaped beam containing fast runaway electrons hits a central anode spot. By a process similar to that of an exploding wire, a superheated liquid is transferred to a more stable twophase system, consisiting of micron size particles immersed in a dense gas phase at high temperature. The particles are ejected ahead of an ionizing plasma wave released form the formed globule. The positively charged particles, indicated by a broken arrow, will sometimes explode by interaction with the strong electron emission from cathod. They are then observed as hot spots emitting x-radiation from highly stripped atoms. Hot spots were

originally observed in the neighbourhood of the anode tip, but later on at different positions in the gapo, also off axis. It is noteworthy that those spots with the sharpest contours often appear in the cathode region. When the dense, expanding wave A_2 immerse in the cathode emission, the bridged gap become conducting and the electrical breakdown follows immediately at t_4.

The pre breakdown model described above is primarily based on published observations of the triggered low inductance vacuum spark, but is applicable also to other modes of the vacuum spark. At very short gap distances, as for the case of contacts to make, 10 to 20 volts is sufficient to set up an electric field at the cosest cathode point strong enough to cause an enormous field electron emission from cathode. This emission produces enough vapor by an explosive interaction at t_1 to fill the gap and cuase breakdown. At this short gap distance $10^{\frac{1}{3}}$ Å, even normal ambient pressure will fulfill the vacuum definition given earlier, and the emitted continuous light is not influenced by the kind of ambient gas in accordance with the model.

Figure 3

Pinhole photographs of single sparks where three distinct x-ray emitting regions can be distinguished.

1. The anode itself which emits characteristic x-rays from electrode material.

2. A diffuse cloud emitting characteristic lines with an extensive unresolved structure of satellite lines arising from x-ray transitions in ionized atoms.

3. A small (3×10^{-3} cm) and very intense region of plasma in which lines corresponding to very high degrees of ionization are produced. Some photographs show two such regions or hot spots.

Figure 4.

Time-resolved total x-ray emission using plastic scintillator in

combination with the 1P21 photomultiplier. The multiplier current was displayed on a double-beam oscilloscope together with the pickup signal (dI/dt) from a Rogowskii coil. The x-ray output reach a maximum at about the time of the most rapid change in dI/dt. This is a soft x-ray burst from bombardment of the anode tip by electrons which partly originates from the trigger spark. About 1,5 microsec later, upon a rapid rise in dI/dt, two complex peaks of x-rays each lasting for about 0.1 microsec are observed. These bursts are much harder than the initial one, and is likewise accompanied by dips in the dI/dt trace.

Figure 5.

X-ray pinhole photograph of hot plasma point 1 mm below the pointed anode tip. The picture is from a single spark and photographed through a beryllium window. The sharp edge of the spot indicates that it is very small compared with the 300 micron pinhole, probably less than 4 microns. The quality and reproducibility of the hot spot depends on electrode geometry and electrical parameters. Fraenkel and Schwob found an optimal value of 80 nH for the inductance of the discharge circuit.

Figure 6.

Spatial resulution of the Kβ (and Kα) radiation from anode tip and the radiation from satellites located to the hot spot approximately 1 mm above the anode tip. The shadow of a tungsten wire placed perpendicular to the discharge axis falls on a curved crystal and on a photographic film. The position of the shadow on a particular line will then depend on the elevation of its source. Experiments using iron electrodes was selected for this and for the following figures.

Figure 7.

The oscillogram on top shows three main deips in the dI/dt waveform indicating three phases (I, II and III) of the discharge. The corresponding x-radiations are energy resulved.
Phase I. Soft x-rays are emitted from electron bombardment of anode

surface.
Phase II. Normal Kα,β and soft x-ray continuum from a faint cloud extending from the anode and into the gap. A contracted luminous plasma originating near cathode propagates very fast toward anode.
Phase III. A somewhat slower, very luminous plasma propagates toward cathode. The main x-ray burst is emitted from a concentrated plasma point.

The steep increase in energy and intensity throughout the phases I to III is remarkable. One further notice the approximate constant delay of 0.5 microsec between the phases.

Figure 8.

Time histories of x-ray signals at different energies. The steep (<2 nanosec) pusles from suprathermal-electrons (>20 keV to > 200 keV) coinsides with the fast thermal component from Fe XXV, and with microwaves in the K-band (≈ 25 GHz). The X-band (≈ 10 GHz) is broad, and the slower thermal components are increasingly tailed toward longer lifetimes, The limetime may be as long as 1 microsec compared with 20 nanosec for the suprathermal component.

Figure 9.

A sketch of a streak photo as viewed through a slit parallel to the discharge axis. Arrow-marks indicate instances of x-ray bursts at time intervalls 7-15 nanosec. These bursts are located to plasma points moving ahead of the luminous plasma front.

Figure 10.

Fastocilloscope traces of He-like lines and hard x-rays compared with characteristic Kα. The He-like lines started 5 nanosec later than Kα, but decayed much faster. The hard x-rays started only 2-3 nanosec later than Kα, but reached its maximum much earlier. The peak become narrower with increased absorber thickness, but the starting time relative to Kα remained the same.

Figure 11.

Vacuum spark spectra of Fe recorded without spatial resolution by Fraenkel and Schwob /12/, and through a slit by Lee /15/. The slit was placed perpendicular to the electrode axis to obtain radiation from the hot spot area and to exclude the normal characteristic x-radiation from the anode tip by axial space resolution. An intense cool-plasma emission at 1.93 Å arises from Fe XVII-XVIII at a temperature of 350 eV. The spectral lines on the short wavelength side of Kβ are from transitions in Fe IX-XVII corresponding to a plasma temperature of ≈ 30 eV. These cool plasmas surrounds the hot plasma points capable of producing H-like Fe XXVI lines at plasma temperatures of 2-3 keV, and more intense He- og Li-like lines from Fe XXIV and Fe XXV respectively.

Figure 12.

K spectrum from exploded Fe wire (≈ 50 microns) due to a 80 nanossec, 10^{12}w relativistic electron puls from a Gamble II generator. About 50 kJ is dissipated to produce a plasma similar to the spatially resulved spark plasma on fig. 11.
Hot plasmas (1,2-1,4 keV) are produced in a series of micropinches along the wire. The estimated electron densities (10^{21} cm^{-3}) and the distribution of ionization stages (Fe fXXIV-XXVI) compares well with the hot plasma points formed in vacuum sparks. The micropinches are surrounded by cool plasmas as in the case of a vacuum spark, but at a somewhat lower temperature (≈ 150 eV). As one should expect, the controllable conditions for wire explosions gives hot plasma temperatures and ionization stages with far better reproducibility than in the case of the rather erratic spark.

Figure 13

Time resolved x-ray emission from vacuum spark plasma and electrodes. Two complex x-ray bursts appear during the first quarter cycle of discharge (1.5 nanosec), and consistently separated in time by 400 nanosec. An analysis of the first complex burst using higher time resolution and slit to select only interelectrode x-ray emission,

reveal 5 nanosec bursts. The complex bursts occurs more regularly than the highly localized x-ray emission on Figure 14, which appears only in one in about three discharges.

Figure 14.

The electrode arrangement at Figure 14 a involved a pointed upper anode and a cylindrical flat topped cathode at an interelectrode spacing of 5 mm. This arrangement gave off-axis hot spots as shown on Figure 14 b and 14 c. The spots observed near cathode were often the most intense and well developed ones. The electrode system on Figure 14 d with a truncated, conical lower cathode, and a skirted top anode gave on-axis plasma points. Figure 14 e shows four hot points from a discharge. On figure 14 f the polarity is reversed, and a single hot spot is observed just above the anode tip as in the original experiments by Cohen et al. /11/ and Fraenkel et al. /12/.

Figure 15.

Figure 15 a and 15 b are pinhole photographs of the same discharge, taken simultaneously with cameras set up on opposite sides of the vacuum spark so that the same event could be photographed through different filters. The object was to discriminate spatially between "optical" transitions from Fe XXV and screened Kα-type emissions. Figure 15 a involves the total emission from 1.49 to 2 Å, whereas Figure 15 b is limited to the narrow band from 1.89 to 2 Å and therefore exclude the emission from highly ionized species from Fe XXIV, Fe XXV and Kβ as seen from Figure 11. The intensity of the hot spot farthest away from the anode tip is reduced in intensity by about 85%. The remaining 15% is emitted by partly screened Kα radiation in Fe XX and in lower ionization stages.

Figure 16.

Vacuum breakdown is initiated by bombarding the anode with focused electron beams from an electron gun at different intensities (q). The oscillographic recordings shows the electrode gap current vs. delay time τ of this current rise with respect to the beginning of the puls

from the gun. At intensities q ≈ 10^6 w/cm^2 (Figure 16 a), the delay time τ varies as q $\Gamma\tau$ = const. At intensities above 10^6 w/cm^2 an anomaleous pre-puls appeared (Figure 16 b) before the steep current rise leading to breakdown. At still higher intensities, the prepuls grows and lead directly to breakdown (Figure 16 c).

Figure 17.

Figure 17 a shows how the pinch radius (r) reach a minimum approximately 25 nanosec before the dI/dt dip and the x-ray peaks. The hard x-ray emission (hν > 100 keV) and the characteristic Kα lines of Fe II-XV are supposed to be due to interaction on anode surface of a superthermal electron beam. They appear 3-5 nanosec before emission of the resonnant lines of He- like Fe XXV and x-rays at 25-200 keV. The two last mentioned x-ray emission groups are thermalized and ascribed to the formation of a plasma point which coincide within ± 10 nanosec with the minimum on the dI/dt curve. The relative temporal positions of signals on Figure 17 a-f varies somewhat from discharge to discharge, and the quoted differences are an average from 100 separate discharges.

Figure 18.

An analysis of dust particles which adhered to the top window of apparatus showed a preponderance with dimensions < 10 microns, which closely matches the size of "hot spots" measured with the x-ray pinhole camera. These particles compares well with those found in the debris collected from a screen placed in the neighbourhood of an exploding wire.

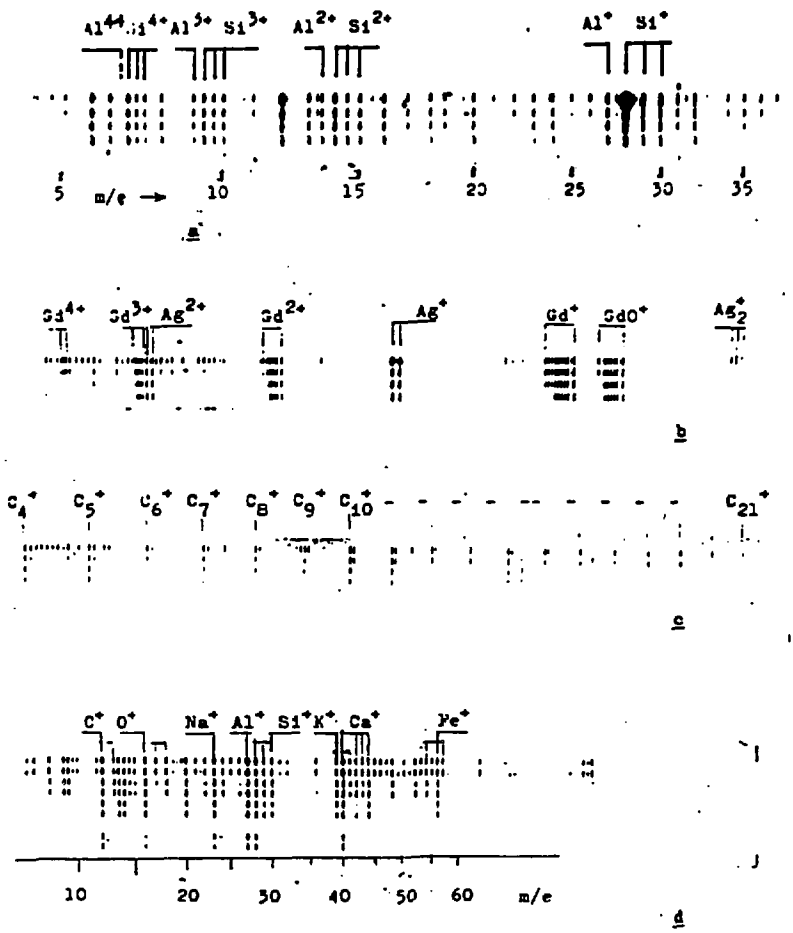

Figure 1. Mass spectra from AEI MS702 double-focussing mass spectrograph with r.f.vacuum spark and Ilford Q2 photoplate registration.

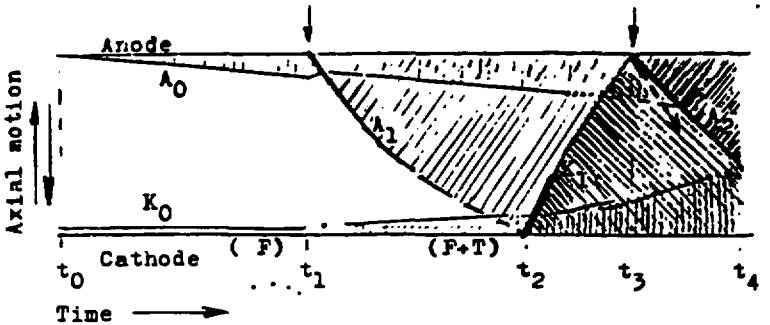

Figure 2. Sketch indicating the time resolved movements of plasma waves to fill det gap by cooperative processes.

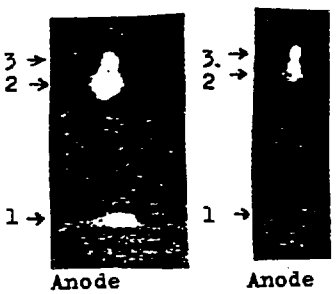

Figure 3.
Pinhole photographs of single sparks Cohen et al. /11/.

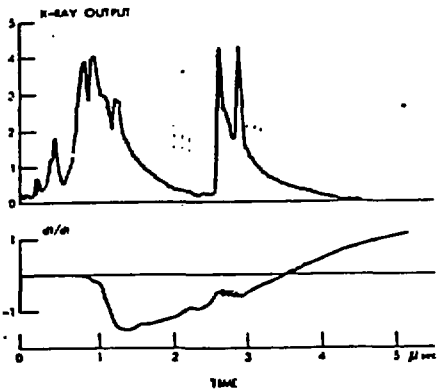

Figure 4.
Time variation of the photo multiplier x-ray current and dI/dt during a typical discharge. Iron electrodes. Cohen et al. /11/

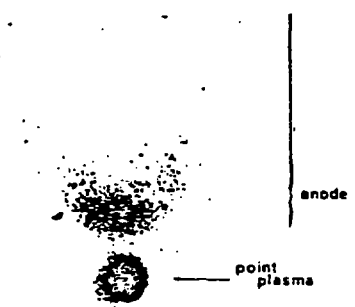

Figure 5.
Pinhole x-ray photograph of a single spark. Fraenkel et al. /12/

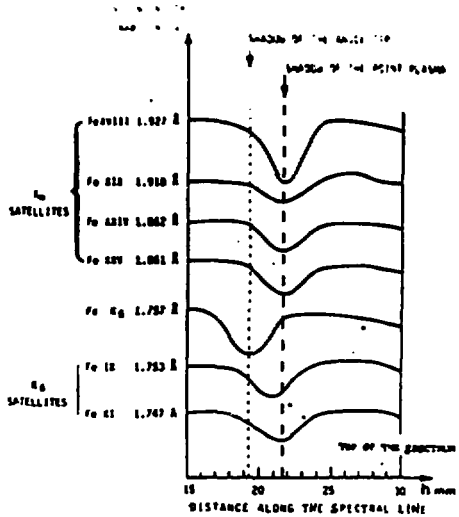

Figure 6.

Determination of x-ray source location suing the shadow of a tungsten wire. Klapisch et al. /13/

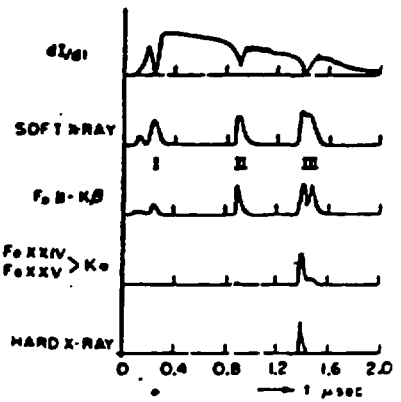

Figure 7.

Oscillograms showing the dI/dt waveform and x-ray spectral signals from the scintillation detector. Lee et al. /6/.

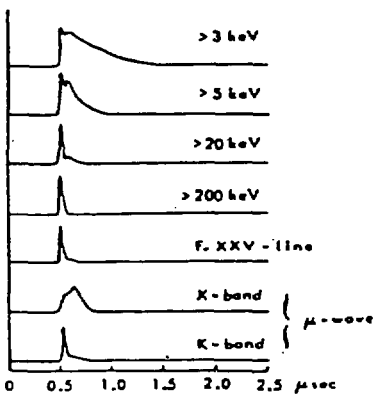

Figure 8.

Time histories of x-ray and micro-wave signals. Lee /14/.

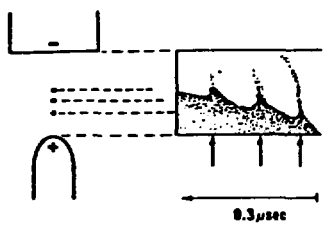

Figure 9.

A sketch of a streak photograph taken through a slit oriented parallel to the discharge axis, and the resulting point plasmas. Arrow marks indicate instances of x-ray bursts. Lee /15/.

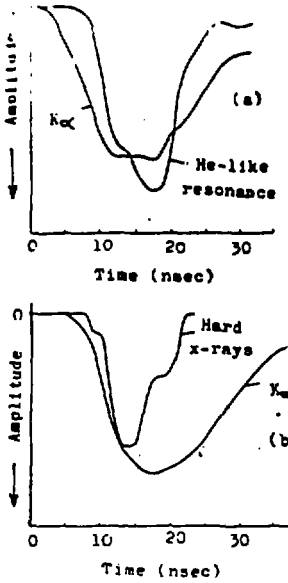

Figure 10.

Fast oscilloscope traces of Kα simultaneously with He-like line (a), and with hard x-rays (b). Cilliers et al. /9/.

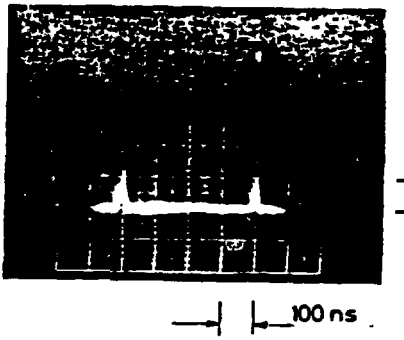

Figure 13.

Time history of x-ray emission from the vacuum spark. Negus et al. /16/.

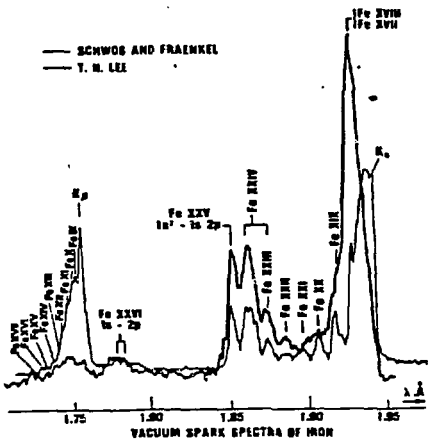

Figure 11.

Compairison of vacuum spark spectra of Fe recorded without spatial resolution by Fraenkel et al. /12/, and through a slit by Lee /15/. Burkhalter et al. /3/

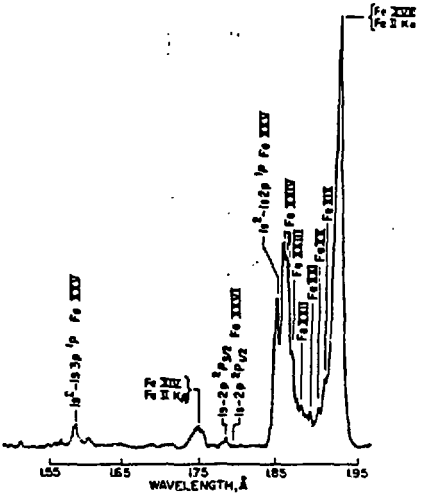

Figure 12.

Exploded-Fe-wire from Gamble II. Burkhalter et al. /3/

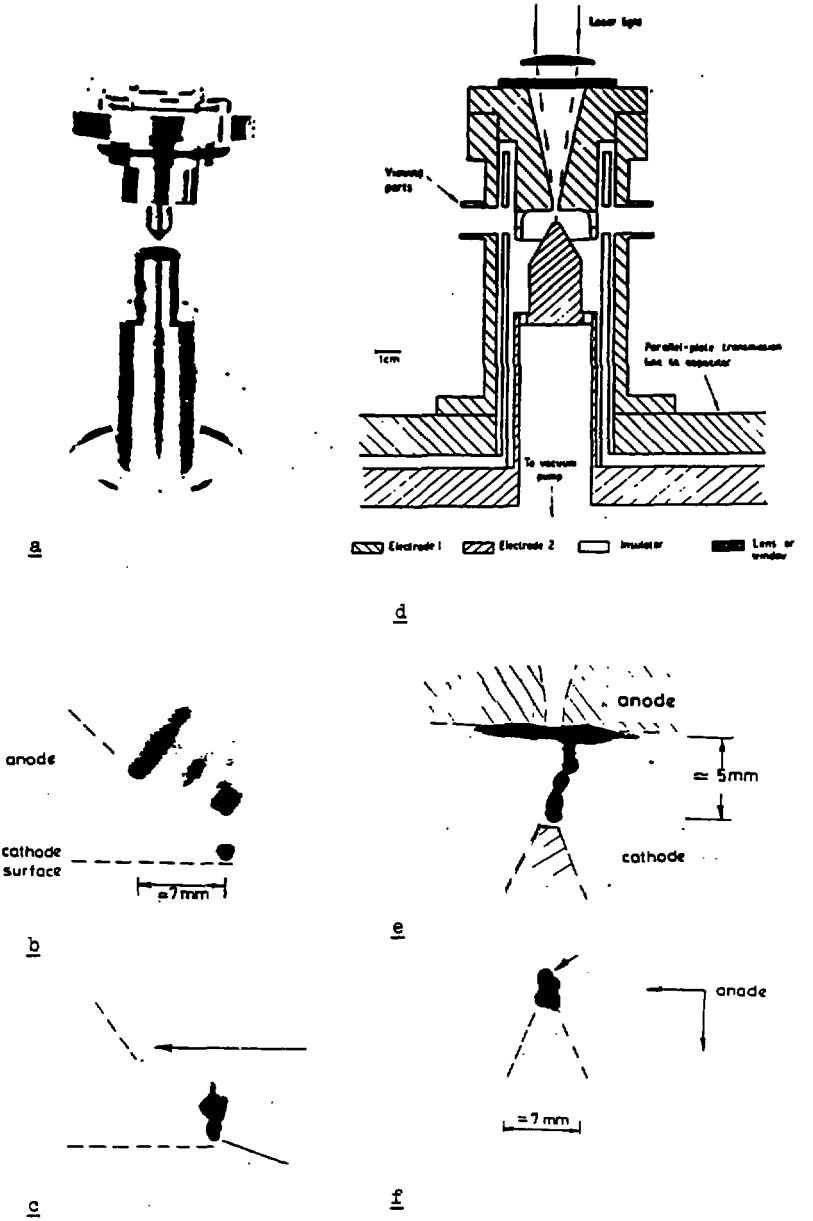

Figure 14.

X-ray pinhole photographs of different types of hot plasma point formation. Negus et al. /16/.

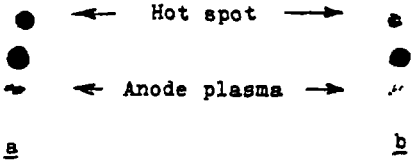

Figure 15.
X-ray pinhole photographs taken through a Ross filter system. Negus et al. /16/.

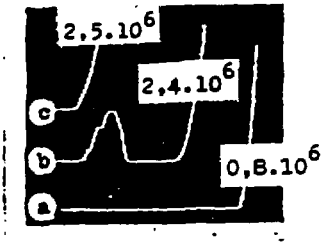

Figure 16.
Oscilloscope traces of electrical processes in vacuum gap during bombardment of anode with an electron beam 10^6 w/cm^2. Poshekonov et al. /17/.

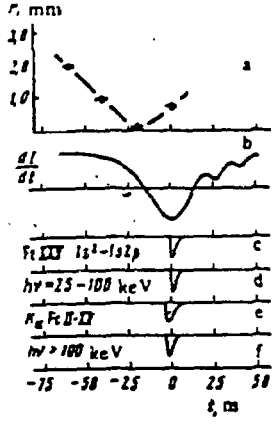

Figure 17.
Occurrence of minimum pinch radius (r) and dI/dt dip, related to the times of x-ray bursts. Veretennikov et al. /10/.

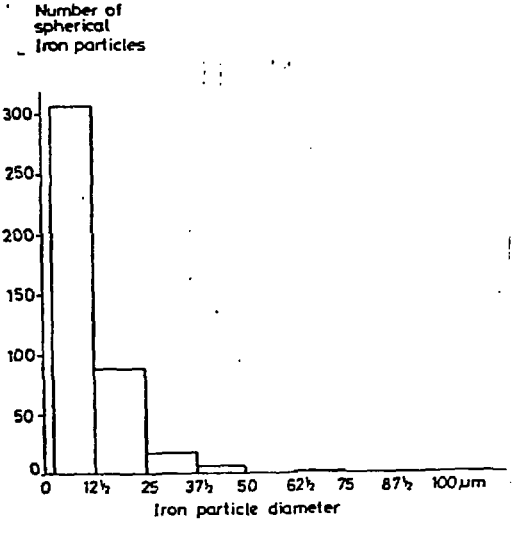

Figure 18.
Distribution of iron particles formed during a number of sparks. Negus et al. /16/.

«The Institute's mandate is to conduct research and development, analyses etc. within the field of energy, including nuclear research, and other fields particularly suited to the Institute's competence».

Energy oriented activities:

- Nuclear energy
- Petroleum technology
- Renewable energy technologies
- Energy conservation
- Energy systems analyses

Special activities:

- Process development
- Process modelling and -simulation
- Reservoir technology
- Fluid- and gas flow technology
- Process control and -supervision
- Nuclear fuel technology
- Safety analyses
- Materials technology
- Radioisotopes for medical- and industrial application
- Physical- chemical analyses
- Radiation instruments and -recording

The Institute is the owner and operator of the Halden Boiling Water Reactor. R & D work connected to the operation of the reactor started in 1958 and is sponsored through an OECD international agreement.

The Institute has 500 employees, 300 at Kjeller and 200 in Halden.

Institute for
energy technology
Box 40
N-2007 Kjeller
Norway
Telephone (02) 71 25 60
Telex 76361 energ n

Institute for
energy technology
Box 173
N-1751 Halden
Norway
Telephone (031) 83 100
Telex 76335 energ n